Update of the $\pi N \to \eta N$ and $\eta N \to \eta N$ partial-wave amplitudes

Mijo Batinić, Ivan Dadić, Ivo Šlaus, Alfred Švarc

Ruđer Bošković Institute, Zagreb, Croatia

B.M.K. Nefkens

University of California Los Angeles USA

and

T.-S.H. Lee

Physics Division, Argonne National Laboratory, Argonne, Illinois, USA

A three-channel, multi-resonance, unitary model developed in 1995 is used to determine the $\pi N \to \eta N$ and $\eta N \to \eta N$ amplitudes using as input the latest data for the dominant S_{11} πN elastic scattering partial wave following suggestions of Prof. G. Höhler. The sign error in the numerical evaluation of the dispersion integral in the original publication is eliminated. The remaining weighted data set for the $\pi N \to \eta N$ total and differential cross sections is used as in the original publication. The correction of the numerical error influences the ηN cusp effect and improves the quality of the fit to the input data. However, our new result for the ηN scattering length, $a_{\eta N} = (0.717 \pm 0.030) + i(0.263 \pm 0.025)$ fm, is a sole consequence of the correction of the S_{11} input and suggests that the ηd system is unbound or loosely bound.

I. INTRODUCTION

A three-channel, multi-resonance, unitary model, based on the formulation developed in Ref. [1], has been applied in Ref. [2] to perform a partial-wave analysis (PWA) using the Karlsruhe-Helsinki PWA (KH80) [3] as input for the πN elastic scattering, and the weighted total and differential cross section data for the $\pi N \rightarrow \eta N$ reaction. The partial-wave amplitudes for the $\pi N \rightarrow \eta N$ and $\eta N \rightarrow \eta N$ transitions are the predictions of the model. Using the ηN elastic scattering partial-wave amplitudes thus obtained, the ηN S-wave scattering length $a_{\eta N}$ has been extracted. In Ref. [4] it was stressed that the multi-resonance approach is essential in determining the value for $a_{\eta N}$. The ηN scattering length reported in that article as well as the value given in Ref. [5] are sufficiently large to imply that the ηd bound state might exist as suggested by several theoretical predictions [6,7,8].

The purpose of this paper is twofold: a. to improve the strongly disputed πN elastic input in the S_{11} partial wave near η production threshold, and b. to correct a numerical sign error [15] in the previous analyses in Refs. [2,4]. We shall show that correcting a sign error in the numerical evaluation of the dispersion integral changes somewhat the predictions of the model, but the crucial parameter for the near η thereshold calculation of other processes - ηN S-wave scattering length is strongly changed due to the correction of the near ηN threshold πN elastic input only.

A sign error in the numerical evaluation of the dispersion integral Eq.(19) of [2], see [15], has influenced the shape and numerical values of all predicted partial wave amplitudes. We give the corrected values with the dotted lines in the Figs.3-10. The numerical values for the resonance parameters and the ηN S-wave scattering length are given in Table 1. We have found that the correction of this error influences the shape of the cusp effect, but leads to a better fit to the input πN data. However, as it can be seen from Table 1. the ηN S-wave scattering length stays rather high.

As a second part of our article we have introduced a new physical input by changing the controversial πN elastic S-wave near η production threshold. The πN elastic scattering input (KH80) that was used in the analyses of Refs. [2,4] has been critically reviewed recently [9,10]. It was concluded that the S-wave part of the KH80 solution can be considerably improved in the energy range below η production threshold [9,10]. It has been shown within an one-resonance model that the suggested modifications in the πN elastic scattering input introduce about 20 % change in the real part of the ηN S-wave

scattering length [11,12]. We expect a similar change in a multi-channel, multi-resonance model. Since the real part of the ηN S-wave scattering length is the basic input for the theoretical investigations of the possible existence of the η-light nuclei bound states [6,7,8], a new fit with the improved πN input is clearly needed in making progress in this direction. We have employed the model of Ref. [2] to carry out a new partial-wave analysis using the improved πN input, as suggested by G. Höhler [13].

With the correct treatment of the dispersion integral and the use of the improved πN input, our new partial-wave analysis yields $a_{\eta N} = (0.717 \pm 0.030) + i(0.263 \pm 0.025)$ for the ηN S-wave scattering length. Its real part is close to the lowest value, $\mathrm{Re}(a_{\eta N})$=0.7, for the existence of an ηd bound state as predicted in Refs. [7,8]. Therefore, the probability of producing an ηd bound state by using various intermediate energy nuclear reactions is greatly reduced.

In section II, we briefly review the employed formalism. The input data used in this analysis is described in section III. In section IV, we present figures showing the fit to the corrected and new πN elastic scattering input, as well as the resulting amplitudes for all transitions between πN, ηN and an effective $\pi^2 N$ quasi two-body channel. Accordingly, the extracted resonance parameters and the S-wave scattering length are given in Tables 1 and 2.

II. FORMALISM

The formalism used in this work originated from the old CMU-LBL analysis [1], and was presented fully in Ref. [2]. However, a sign error was made in the numerical evaluation of the dispersion integral, Eq.(19) of Ref. [2], such that the imaginary part of the dispersion integral was taken incorrectly on the lower half of the Riemann sheet. In Fig.1, the dashed line shows our old solution [2], and the dotted line is the solution obtained after the sign error is corrected. The data (dot points) of the KH80 solution near η production threshold are also displayed . As can be seen in Fig.1. the numerical error in the evaluation of the dispersion integral has changed the shapes of real and imaginary parts of the S-wave amplitude. In addition, the signs of the first derivatives of real and imaginary parts also reverse in the region near the threshold. The solid curves, which are obtained after updating the controversial πN elastic S_{11} input for the energies up to η production threshold, are in agreement in shape with the results of the single resonance

model of Bennhold and Tanabe [17] (dashed line). The differences in magnitudes reflect the importance of using a multi-channel and multi-resonance approach, as stressed in Ref. [4].

III. THE NEW INPUT

As we have already mentioned in section I, there are sufficient reasons to improve the previously used KH80 solution by using a better determined S_{11} partial wave amplitude. It was pointed out in Refs. [9,10] that the KH80 solution in the S-wave is too high when the new data are included. A complete new analysis using the Karlsruhe-Helsinki dispersion relation approach has however not been done. Therefore, a compromising approach is to use the following recipe [13]: use the KH80 single-energy solution everywhere with the exception of the S_{11} partial wave below 1500 MeV total c.m. energy where the SM95 single-energy solution from Virginia Polytechnic group [14] should be used. This is adopted in this work. We have chosen not to compare the full SM95 solution with the KH80 because they have established quite different number of resonances per partial wave. That, of course, influences the number of bare propagator initial terms. In addition, KH80 goes somewhat higher in energy then SM95 because of analytical constraints built into it. The differences due to this modification are shown in Fig.2. The open dots represent the KH80 single-energy solution, while the full dots represent SM95 single-energy solution. The transition from one solution to the second one is smooth, as can also be seen from the Fig.2. Full and dashed curves serve only to guide the eye. The SM95 solution differs significantly from the KH80 below 1500 MeV c.m. energy, so distinct consequences upon the ηN scattering length in S-wave are expected. We mention here that because of the nature of the model, the fit to other partial waves will also be influenced by this modification of the input in S-wave.

IV. RESULTS AND CONCLUSIONS

The extracted ηN S-wave scattering length is given in Tables 1 and 2, together with the extracted resonance parameters in the notation of Ref. [2], and separately in Fig.3. The determined new $\pi N \rightarrow \pi N$, $\pi N \rightarrow \eta N$, $\eta N \rightarrow \eta N$ and $\pi N \rightarrow \pi^2 N$ partial wave amplitudes are the solid curves shown in Figs. 4-11. The old results (dashed curves) from

3

Ref. [2], as well as the results after eliminating the afore described numerical error (dotted lines) are also displayed for comparison. We conclude:

1. The $\pi N \to \eta N$ and $\eta N \to \eta N$ amplitudes for the solution with the KH80 input, but corrected for the sign error, are closer to the final solution with the modified πN elastic S_{11} input. However, the important ηN S-wave scattering length is drastically changed from $(0.91 \pm 0.030) + \mathrm{i}\,(0.29 \pm 0.040)$ to $(0.71 \pm 0.030) + \mathrm{i}\,(0.263 \pm 0.023)$ when the uptake of the S_{11} input is introduced. That changes the former, erraneous conclusion that the ηd bound state is likely to exist to the correct statement that the ηd bound state is either nonexistent or losely bound [7,8].

2. The quality of the overall fit to the input data is improved.

   a. The fit (Figs. 4 and 5) to the new πN elastic scattering input is improved; particularly for the S-wave (see Fig. 4). It appears that the correction of the error in the evaluation of the dispersion integral, Eq.(19) of Ref. [2], helps the improvement of the fit.

   b. The quality of the fit to all of the experimental total and differential cross section data for the $\pi N \to \eta N$ reaction is practically identical to the fit reported in Ref. [2]. The large differences in higher partial waves (Figs. 6 and 7) do not play a significant role in fitting the existing data that are mainly in the near threshold energy region. The dominant S-wave amplitudes are essentially unchanged.

   c. There are significant differences between the new (solid curves) and corrected old (dotted curves) in the $\eta N \to \eta N$ and $\pi N \to \pi^2 N$ transitions in some partial waves (Figs.8-11). It is interesting to note that the difference in the ηN elastic scattering in S-wave appears to be small, but Fig. 3 shows that the change in the extracted S-wave scattering length is dramatic.

3. Some of the corrected and new values of the resonances parameters (see Tables 1 and 2) are different from the old values reported in Refs. [2]. This mainly reflects the sensitivity of a multi-channel, multi-resonance, unitary approach to the input data, as stressed in Refs. [11].

Acknowledgment

[1] R.E. Cutkosky, R.E. Hendrick, J.W. Alcock, Y.A. Chao, R.G. Lipes, J.C. Sandusky and R.L. Kelly, Phys. Rev., **D20**, 2804 (1979), R.E. Cutkosky, C.P. Forsyth, R.E. Hendrick and R.L. Kelly, Phys. Rev., **D20**, 2839 (1979), R.K. Kelly and R.E. Cutkosky, Phys. Rev., **D 20** 2782 (1979).

[2] M. Batinić, I. Šlaus, A. Švarc and B.M.K. Nefkens, Phys. Rev. C **51**, 2310 (1995).

[3] G. Höhler, in *Charge Exchange Scattering of Elementary Particles*, edited by H. Schopper, Landolt-Börnstein, New Series, Group X, Vol 9, Part 2, Subvolume b, (Springer-Verlag, Berlin, 1983).

[4] M. Batinić, I. Šlaus and A. Švarc, Phys. Rev. C **52**, 1 (1995).

[5] M. Arima, K. Shimizu and K. Yazaki, Nucl. Phys. **A543**, 613 (1992).

[6] R. Bhalerao and L.C. Liu, Phys. Rev. Lett. **9**, 865 (1985).

[7] A.M. Green, J.A. Niskanen and S. Wycech, preprint **nucl-th/9604038**, available at xxx.lanl.gov (1996).

[8] S. Wycech, Contribution to the **Workshop on Physics with the WASA Detector**, Sätra Brun, June 17 - 19, 1996.

[9] G. Höhler, in πN *Newsletter*, edited by G. Höhler, V. Kluge, and B.M.K. Nefkens (University of California), Los Angeles, 1993), No.9, p.1.

[10] G. Höhler and H.M. Staudenmaier, in πN *Newsletter*, edited by D. Drechsel, G. Höhler, W. Kluge and B.M.K. Nefkens (Universität Karlsruhe, Universitätsdruckerei, 1995), No.10, p.7.

[11] M. Batinić, A. Švarc, Few Body Syst. **20**, 69 (1996).

[12] A. Švarc, contribution to the **Workshop on Physics with the WASA Detector**, Sätra Brun, June 17 - 19, 1996.

[13] G. Höhler, private communication, April 96.

[14] Solution SM95 obtained from SAID (June 95): Department of Physics, Virginia Polytechnic Institute and State University, Blacksburg, VA 24061, USA.

[15] The error was discovered by Tom Vrana and T.-S.H. Lee in their test of a general multi-channel, multi-resonance, unitary model developed by T. Vrana, S. Dytman, and T.-S. H. Lee, which was presented as contributions to the proceedings of PANIC, 1996, and CEBAF/INT Workshop on N^*, 1996; to be published.

[16] Particle Data Group: M. Aquillar-Benitez, et al., Phys. Rev. D **45**, S1 (1992).

[17] C. Bennhold and H. Tanabe, Nucl. Phys., **A350**, 625 (1991)

TABLE I. *Resonance parameters of the old and corrected multiresonance model with 4 P_{11} resonances.* The results of elastic πN analyses [1,3,16] are given in the first column. The results of the partial wave analysis of old publication [2] are given in columns 2-6, and the results of this publication, corrected for the sign error, are given in columns 7-11. The values of the old and corrected ηN S-wave scattering lengths are given at the end.

States	Old solution					Corrected solution				
$L_{2I,2J}$	Mass	Width	x_π	x_η	x_{π^2}	Mass	Width	x_π	x_η	x_{π^2}
$\left(^{x_{el}}_{Mass/Width}\right)$	(MeV)	(MeV)	(%)	(%)	(%)	(MeV)	(MeV)	(%)	(%)	(%)
$S_{11}\left(^{38}_{1535/120}\right)$	1542(6)	150(15)	34(9)	63(7)	3(3)	1550(9)	204(39)	39(8)	57(7)	4(3)
$S_{11}\left(^{61}_{1650/180}\right)$	1669(17)	215(32)	94(7)	6(5)	0.2(2)	1659(11)	213(20)	77(9)	13(7)	10(4)
$S_{11}\left(^{9}_{2090/95}\right)$	1713(27)	279(54)	49(21)	2(3)	49(19)	1792(23)	360(49)	35(7)	19(10)	46(10)
$P_{11}\left(^{51}_{1440/135}\right)$	1421(18)	250(63)	56(8)	0(0)	44(8)	1442(17)	438(125)	62(4)	0(0)	38(4)
$P_{11}\left(^{12}_{1710/120}\right)$	1766(34)	185(61)	8(14)	16(10)	76(21)	1718(16)	195(18)	28(20)	5(7)	67(20)
P_{11}	1760(29)	109(32)	11(25)	3(7)	86(22)	1737(11)	159(26)	33(29)	12(9)	55(29)
$P_{11}\left(^{9}_{2100/200}\right)$	2203(70)	418(171)	11(7)	86(7)	3(4)	2136(41)	340(86)	16(5)	83(6)	1(1)
$P_{13}\left(^{14}_{1720/190}\right)$	1711(26)	235(51)	18(4)	0.2(1)	82(4)	1722(19)	247(29)	18(3)	2(2)	80(4)
$D_{13}\left(^{54}_{1520/114}\right)$	1526(18)	143(32)	46(6)	0.1(0.2)	54(6)	1523(8)	133(12)	55(5)	0.1(0.1)	45(5)
$D_{13}\left(^{8}_{1700/110}\right)$	1791(46)	215(60)	4(5)	10(6)	86(9)	1821(23)	141(37)	9(6)	20(5)	71(9)
$D_{13}\left(^{6}_{2080/265}\right)$	1986(75)	1050(225)	9(2)	7(4)	84(3)	2047(65)	507(122)	17(6)	8(3)	75(6)
$D_{15}\left(^{38}_{1675/120}\right)$	1683(19)	142(23)	31(6)	0.1(0.1)	69(6)	1679(9)	152(8)	35(4)	0.1(0.2)	65(4)
$D_{15}\left(^{7}_{2100/310}\right)$	2240(65)	761(139)	8(4)	0.1(1)	92(4)	2216(27)	480(16)	13(4)	0.1(0.3)	87(4)
$F_{15}\left(^{65}_{1680/128}\right)$	1674(12)	126(20)	69(4)	1(0.4)	30(4)	1680(7)	142(7)	67(3)	0.2(0.2)	33(3)
$F_{17}\left(^{4}_{1990/35}\right)$	NF	NF	NF	NF	NF	2256(455)	1926(7444)	3(6)	2(4)	95(9)
$G_{17}\left(^{14}_{2190/390}\right)$	2198(68)	805(140)	19(5)	0.1(0.3)	81(5)	2167(89)	505(274)	14(12)	0.2(1)	86(12)

NF ... not found

ηN **S $-$ wave scattering length** :
$$\begin{cases} \textbf{old} : \ a_{\eta N} = (0.876 \pm 0.047) + i(0.274 \pm 0.039) \\ \textbf{corrected} : \ a_{\eta N} = (0.910 \pm 0.030) + i(0.290 \pm 0.040) \end{cases}$$

8

TABLE II. *Resonance parameters of the corrected and new multiresonance model with 4 P_{11} resonances.* The results of elastic πN analyses [1,3,16] are given in the first column. The results of the corrected partial wave analysis of the publication [2] are given in columns 2-6, and the results of this publication are given in columns 7-11. The corrected and new values of the ηN S-wave scattering lengths are given at the end.

States	Corrected solution					New solution				
$L_{2I,2J}$	Mass	Width	x_π	x_η	$x_{\pi 2}$	Mass	Width	x_π	x_η	$x_{\pi 2}$
$\binom{x_{el}}{Mass/Width}$	(MeV)	(MeV)	(%)	(%)	(%)	(MeV)	(MeV)	(%)	(%)	(%)
$S_{11}\binom{38}{1535/120}$	1550(9)	204(39)	39(8)	57(7)	4(3)	1553(8)	182(25)	46(7)	50(7)	4(2)
$S_{11}\binom{61}{1650/180}$	1659(11)	213(20)	77(9)	13(7)	10(4)	1652(9)	202(16)	79(6)	13(5)	8(3)
$S_{11}\binom{9}{2090/95}$	1792(23)	360(49)	35(7)	19(10)	46(10)	1812(25)	405(40)	32(6)	22(10)	46(9)
$P_{11}\binom{51}{1440/135}$	1442(17)	438(125)	62(4)	0(0)	38(4)	1439(19)	437(141)	62(4)	0(0)	38(4)
$P_{11}\binom{12}{1710/120}$	1718(16)	195(18)	28(20)	5(7)	67(20)	1729(16)	180(17)	22(24)	6(8)	72(23)
P_{11}	1737(11)	159(26)	33(29)	12(9)	55(29)	1740(11)	140(25)	28(34)	12(9)	60(35)
$P_{11}\binom{9}{2100/200}$	2136(41)	340(86)	16(5)	83(6)	1(1)	2157(42)	355(88)	16(5)	83(5)	1(1)
$P_{13}\binom{14}{1720/190}$	1722(19)	247(29)	18(3)	2(2)	80(4)	1720(18)	244(28)	18(3)	0.4(1)	82(4)
$D_{13}\binom{54}{1520/114}$	1523(8)	133(12)	55(5)	0.1(0.1)	45(5)	1522(8)	132(11)	55(5)	0.1(0.1)	45(5)
$D_{13}\binom{8}{1700/110}$	1821(23)	141(37)	9(6)	20(5)	71(9)	1817(22)	134(37)	9(6)	14(5)	77(9)
$D_{13}\binom{6}{2080/265}$	2047(65)	507(122)	17(6)	8(3)	75(6)	2048(65)	529(128)	17(7)	8(3)	75(7)
$D_{15}\binom{38}{1675/120}$	1679(9)	152(8)	35(4)	0.1(0.2)	65(4)	1679(9)	152(8)	35(4)	0.1(0.1)	65(4)
$D_{15}\binom{7}{2100/310}$	2216(27)	480(16)	13(4)	0.1(0.3)	87(4)	2217(27)	481(17)	13(4)	0.2(1)	87(4)
$F_{15}\binom{65}{1680/128}$	1680(7)	142(7)	67(3)	0.2(0.2)	33(3)	1680(7)	142(7)	67(3)	0.4(0.2)	33(3)
$F_{17}\binom{4}{1990/35}$	2256(455)	1926(7444)	3(6)	2(4)	95(9)	2262(470)	2036(8235)	3(6)	2(4)	95(8)
$G_{17}\binom{14}{2190/390}$	2167(89)	505(274)	14(12)	0.2(1)	86(12)	2125(61)	381(160)	18(12)	0.1(0.3)	82(12)

ηN **S − wave scattering length** :
$$\begin{cases} \textbf{corrected} : a_{\eta N} = (0.910 \pm 0.030) + i(0.290 \pm 0.040) \\ \textbf{new} : a_{\eta N} = (0.717 \pm 0.030) + i(0.263 \pm 0.025) \end{cases}$$
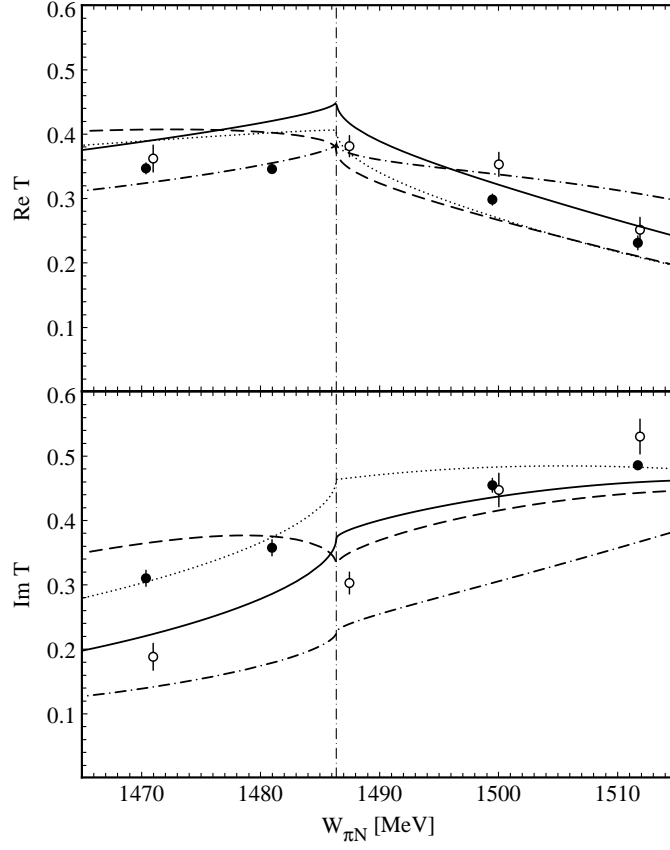
9

FIG. 1. Cusp effect in the πN elastic S_{11} T-matrix near ηN S-wave threshold. Dashed curves are from the solution obtained with the wrong sign in numerical evaluation of Eq.(19) of [2]. Dotted curves are from the solution corrected for the numerical error in the dispersion integral and full curves are from the new solutions (solutions using modified S_{11} πN elastic input). The full dots are from the KH80 single-energy solution near threshold, and the full ones are from SM95 VPI solution. The dash-dotted curves are from the single - resonance model by Bennhold and Tanabe [17] for comparison.

Re T$_{S11}$

Im T$_{S11}$

πN elastic T matrix from: (●) KH80 PWA, (○) VPI SM95 PWA
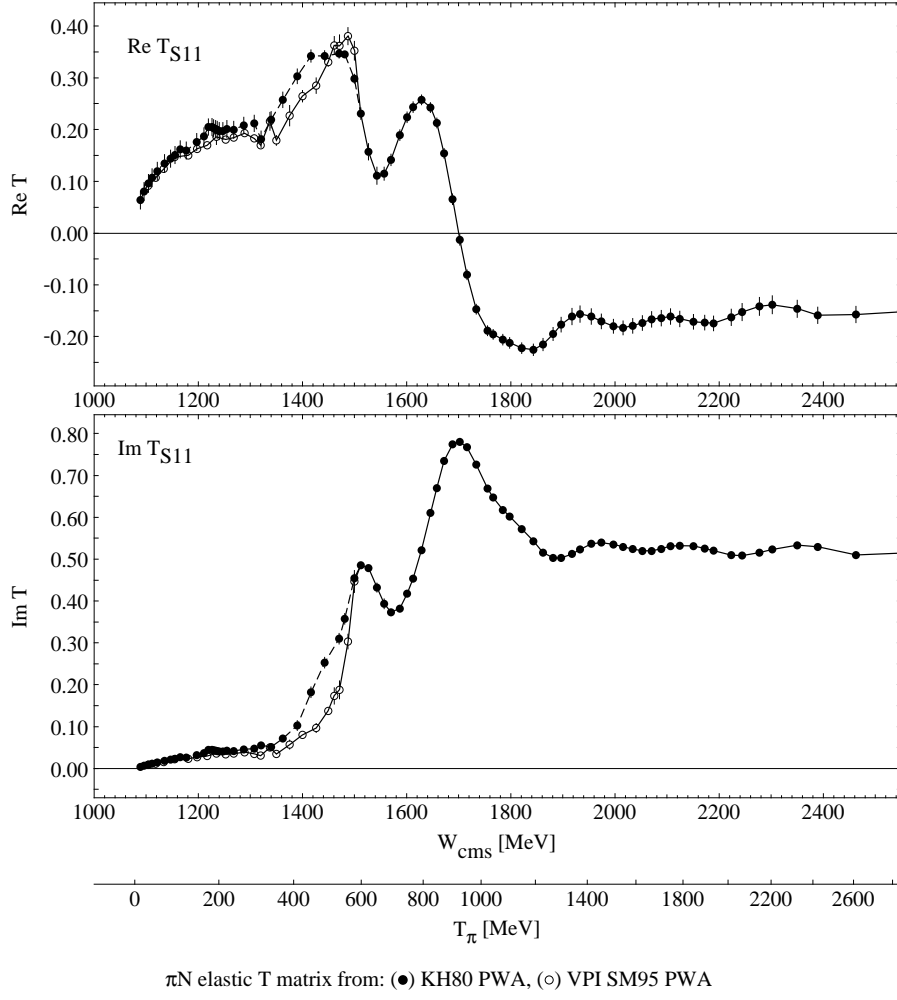
FIG. 2. The new πN elastic scattering input. The full circles represent the old KH80 solution. The open circles (introduced in the S-wave only) represent the replacement of the single energy KH80 solution with the single energy SM95 solution. Full and dashed lines serve only to guide the eye.
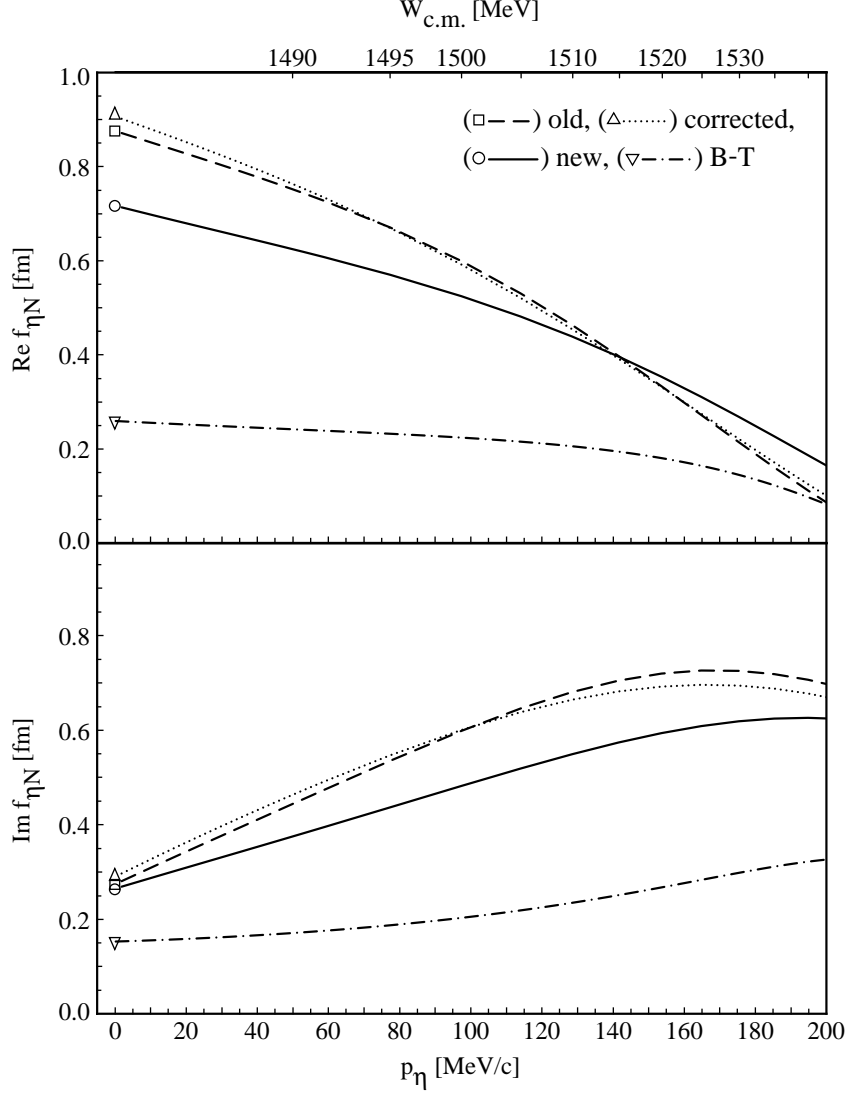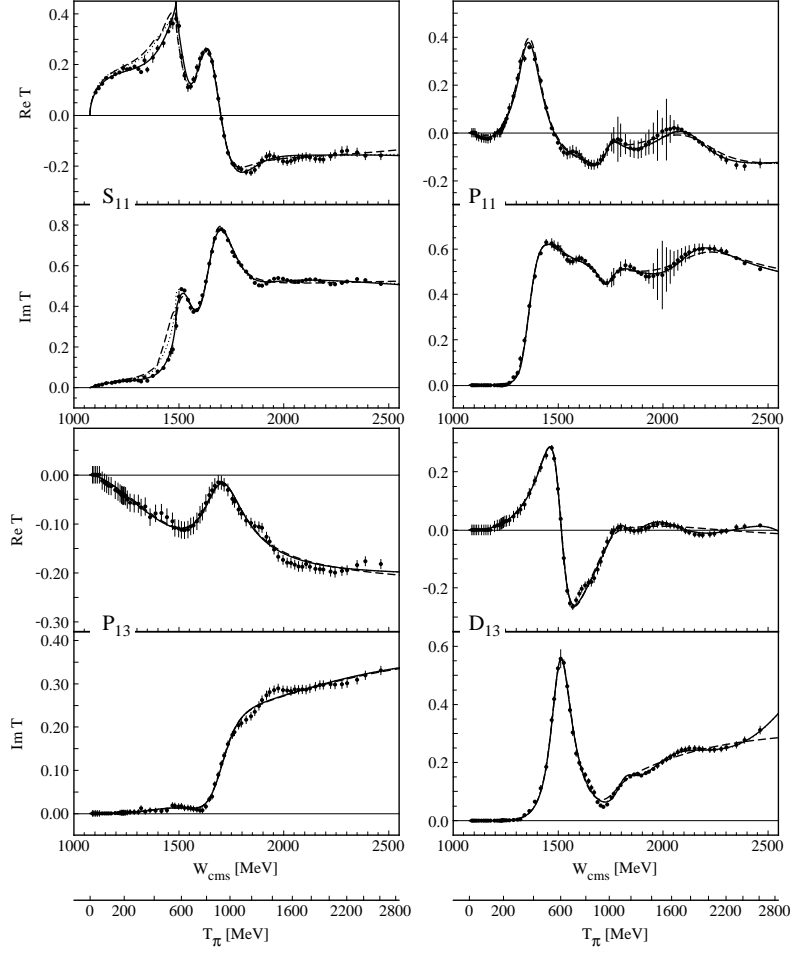
FIG. 3. The dependence of the ηN S-wave scattering amplitude defined as $f_0(p) = T_0^{\eta N \to \eta N}(p)/p_\eta$ upon the η momentum. The lines have the same meaning as in Fig.1.

πN elastic T matrix from: (– –) old, (········) corrected, and (———) new solution;
(●) KH80 PWA (VPI SM95 PWA in S11 for W < 1500 MeV).

FIG. 4. The πN elastic scattering amplitudes in S_{11}, P_{11}, P_{13} and D_{13} partial waves. The filled circles are the single-energy πN elastic scattering amplitudes given in Ref. [3] combined with the SM95 [14] for the S-wave below 1500 MeV c.m. energy. The dashed curves are the result of the three coupled channel multiresonance model of Ref. [2] with the number of resonances given by the PDG [16]. The dotted line is the result of the same model with the corrected numerical error in the evaluation of the dispersion integral. The full line is the result of the same model, but with the afore described modification of the πN elastic S_{11} T-matrices data.
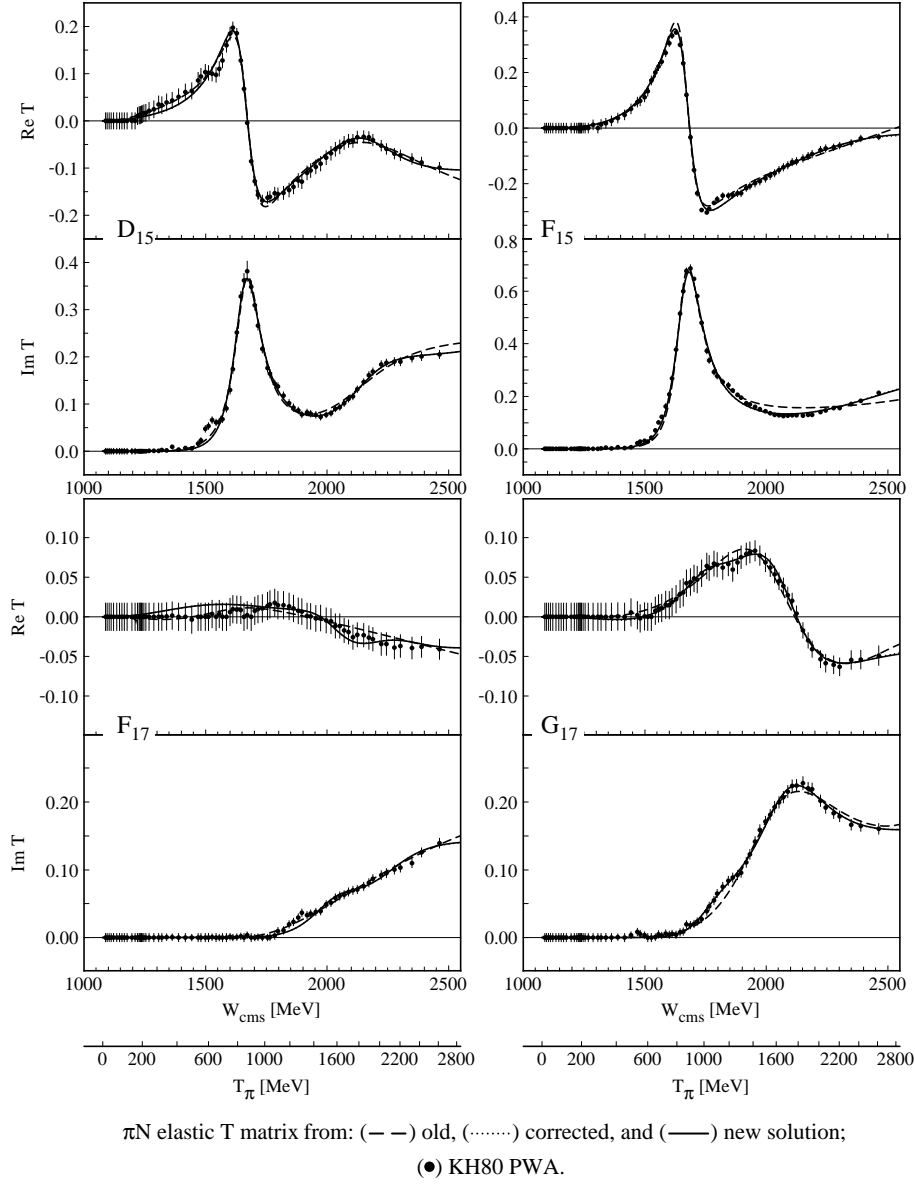
13

πN elastic T matrix from: (— —) old, (·······) corrected, and (———) new solution; (●) KH80 PWA.

FIG. 5. The πN elastic scattering amplitudes in D_{15}, F_{15}, F_{17} and G_{17} partial waves. The filled circles are the single energy πN elastic PWA given in Ref. [3]. The meaning of the different curves is given in the caption of Fig.4.
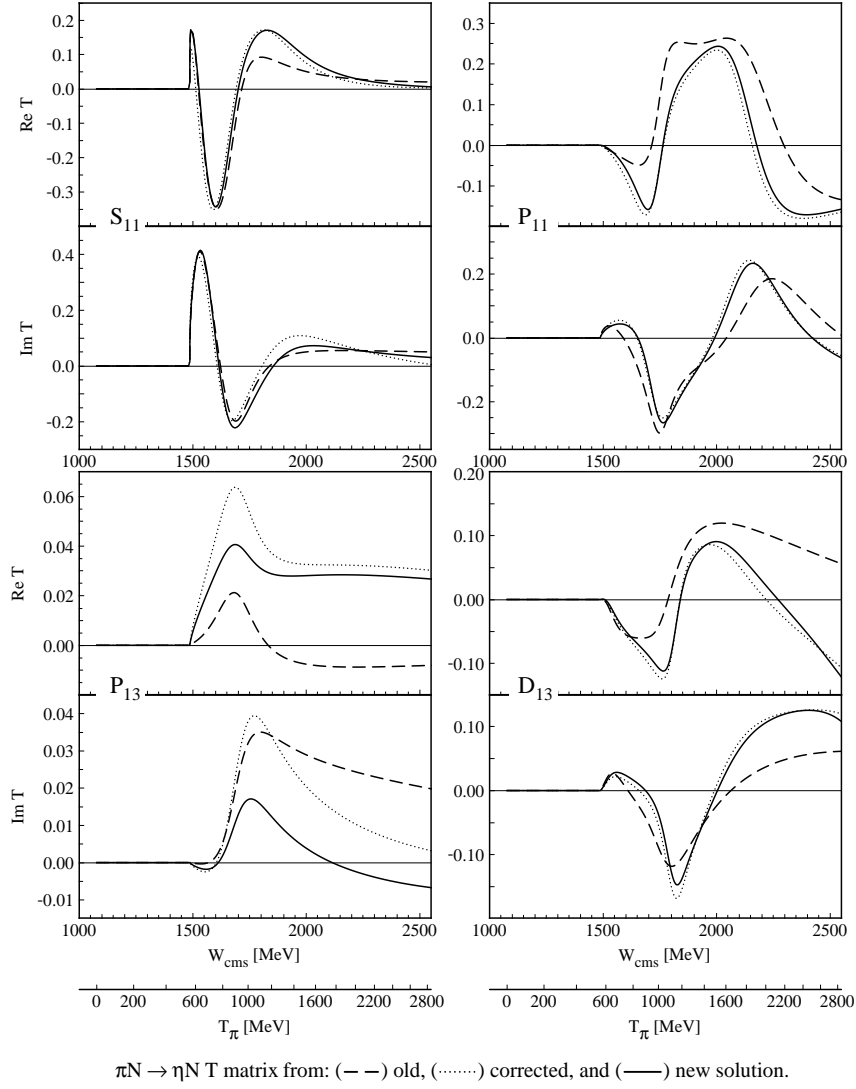
FIG. 6. The $\pi N \to \eta N$ amplitudes in S_{11}, P_{11}, P_{13} and D_{13} partial waves. The meaning of the different curves is given in the caption of Fig.4.

15

$\pi N \rightarrow \eta N$ T matrix from: (− −) old, (········) corrected, and (——) new solution.
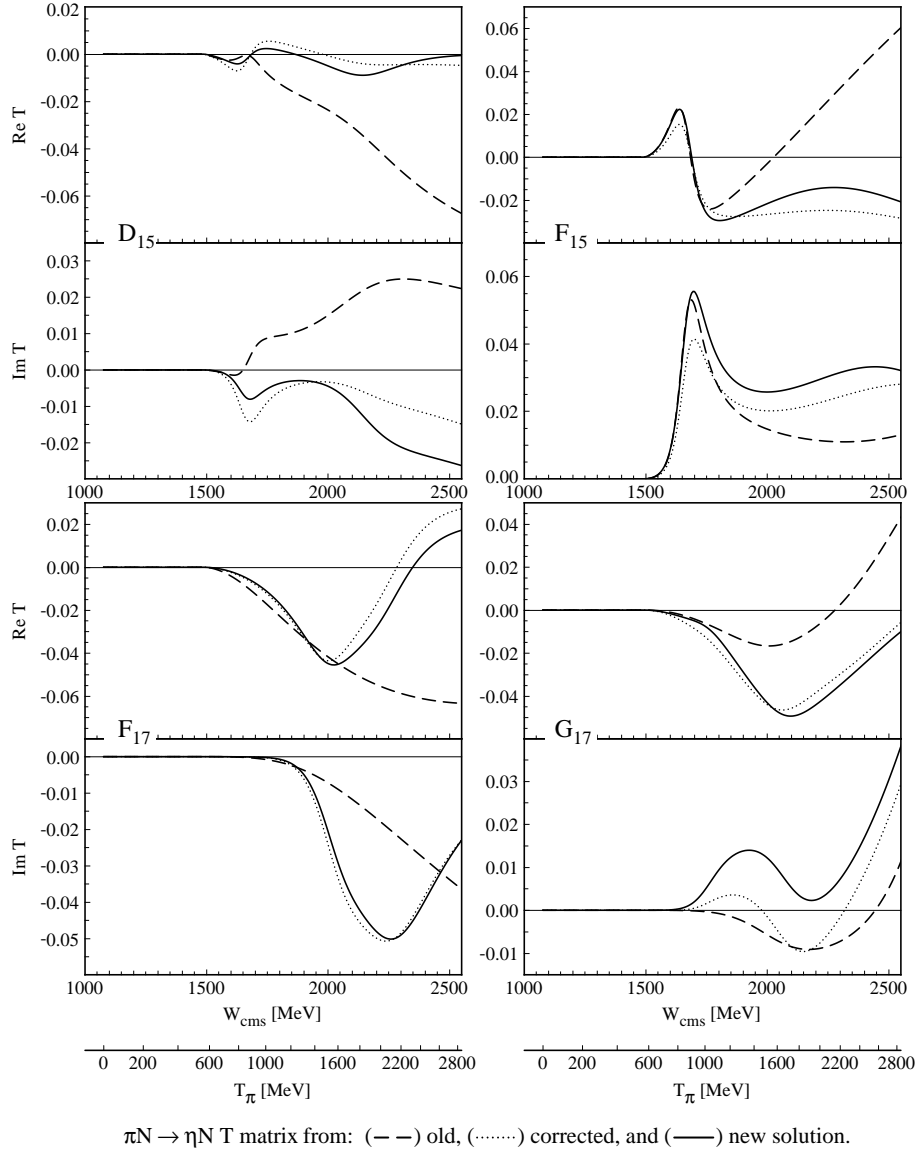
FIG. 7. The $\pi N \rightarrow \eta N$ amplitudes in D_{15}, F_{15}, F_{17} and G_{17} partial waves. The meaning of the different curves is given in the caption of Fig.4.
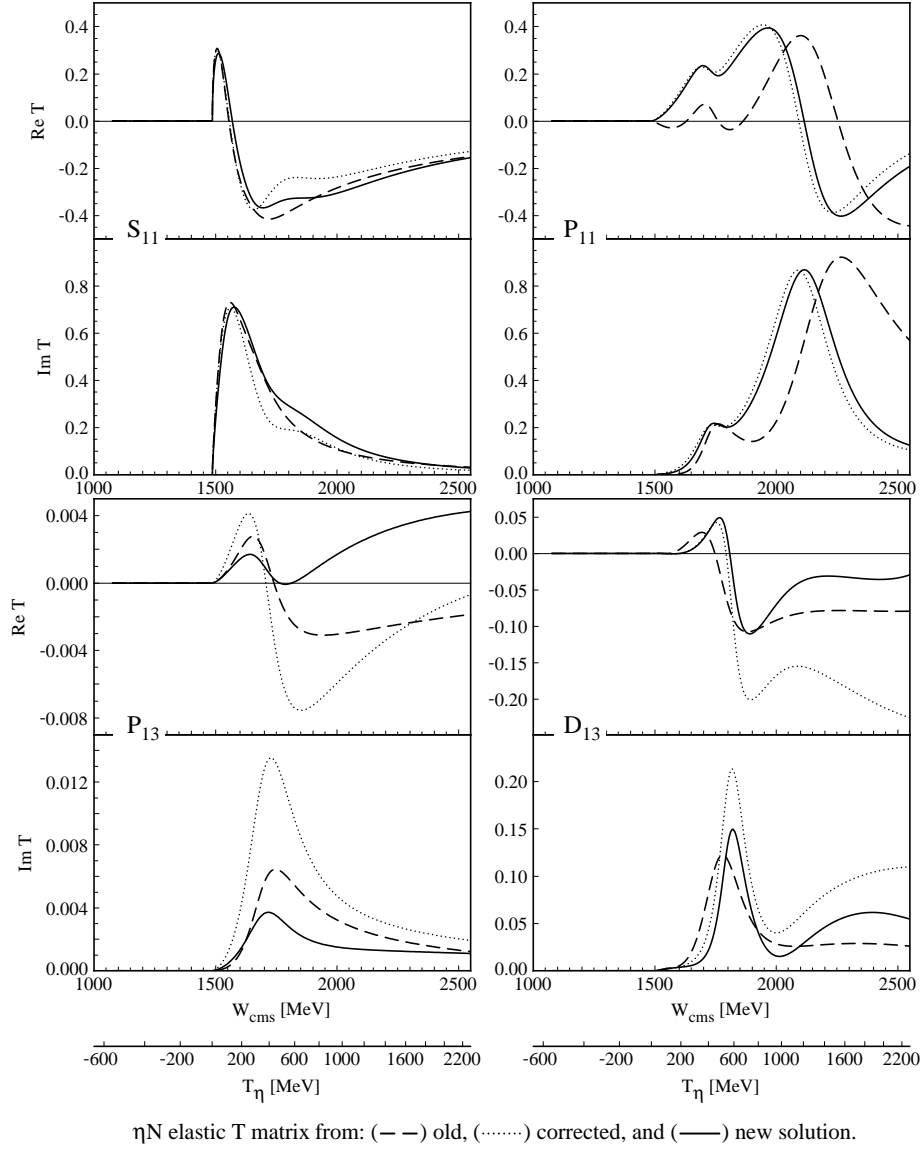
ηN elastic T matrix from: (— —) old, (········) corrected, and (———) new solution.

FIG. 8. The ηN elastic scattering amplitudes in S_{11}, P_{11}, P_{13} and D_{13} partial waves. The meaning of the different curves is given in the caption of Fig.4.
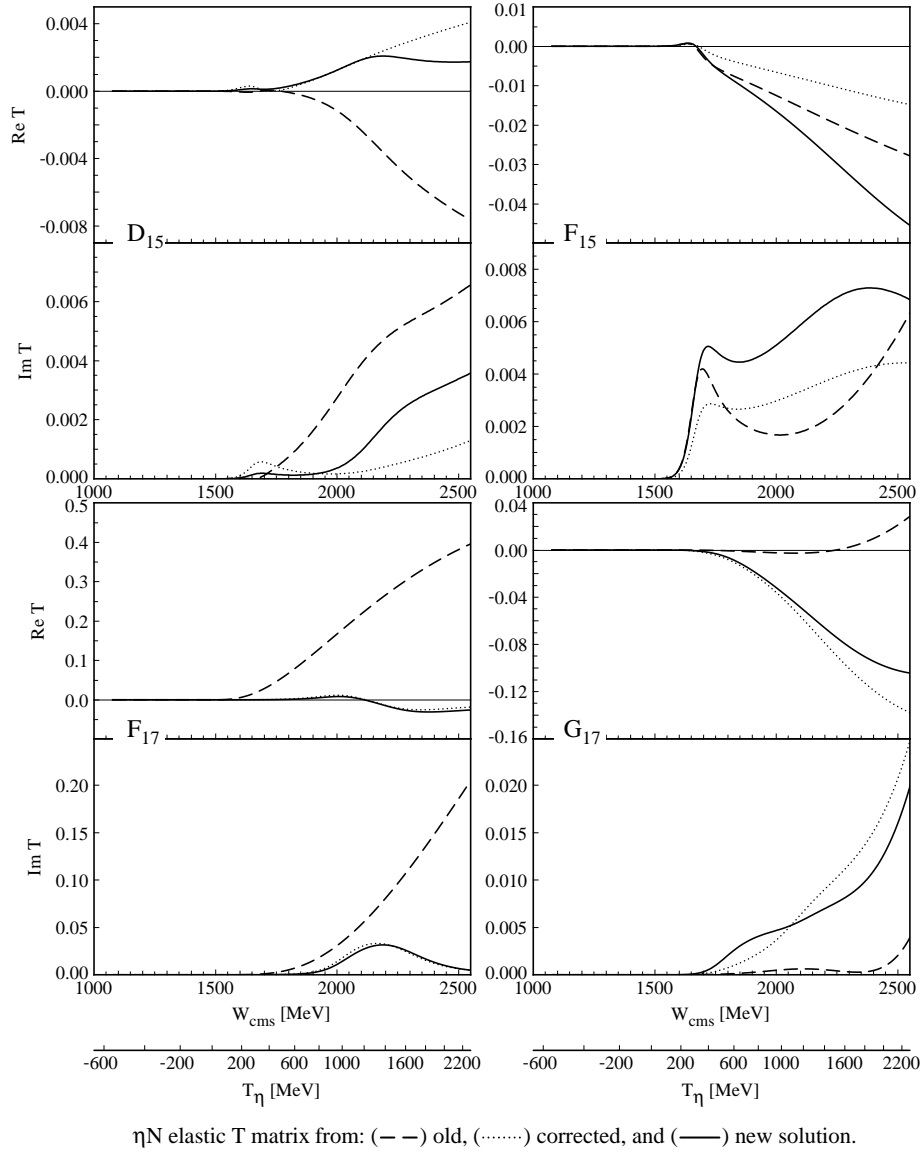
ηN elastic T matrix from: (— —) old, (·······) corrected, and (———) new solution.

FIG. 9. The ηN elastic scattering amplitudes in D_{15}, F_{15}, F_{17} and G_{17} partial waves. The meaning of the different curves is given in the caption of Fig.4.

18

$\pi N \rightarrow \pi^2 N$ T matrix from: (— —) old, (·······) corrected, and (——) new solution.
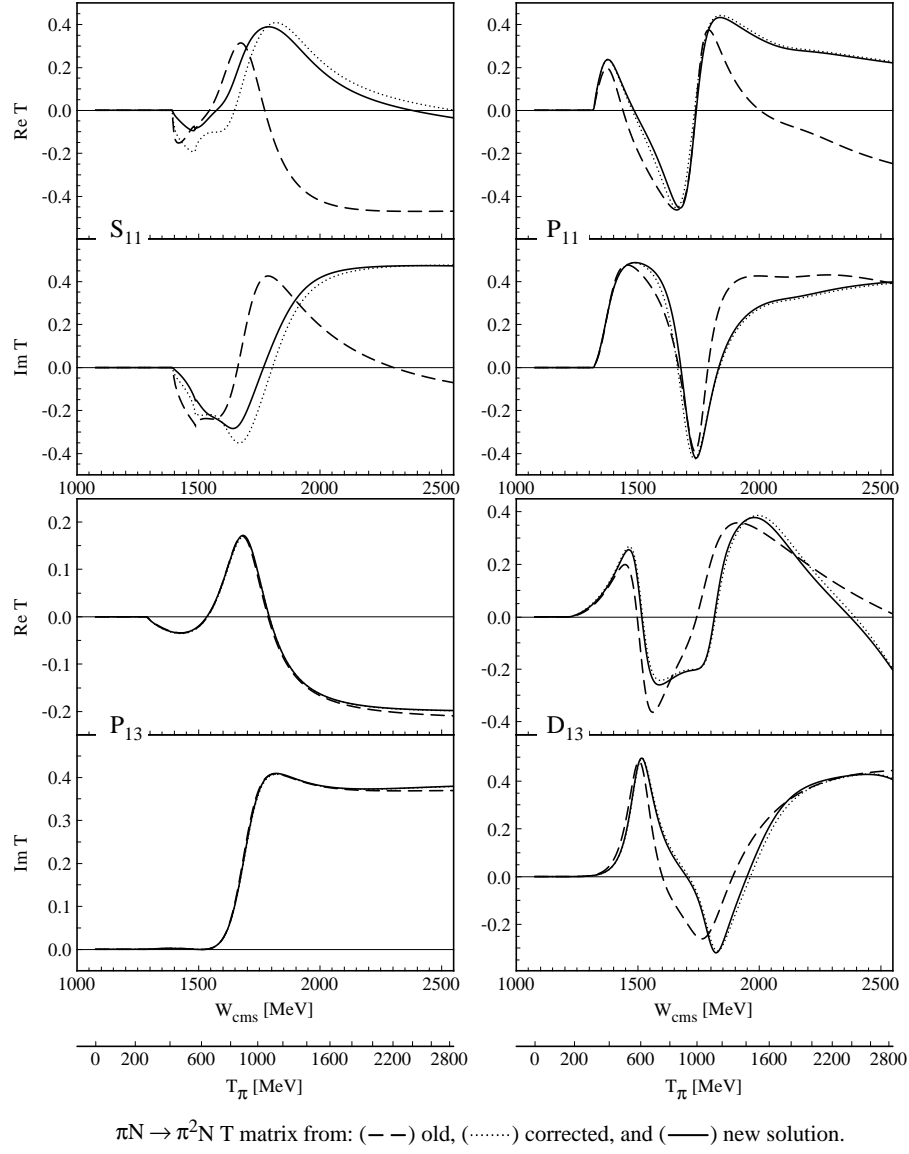
FIG. 10. The $\pi N \rightarrow \pi^2 N$ amplitudes in S_{11}, P_{11}, P_{13} and D_{13} partial waves. The meaning of the different curves is given in the caption of Fig.4.
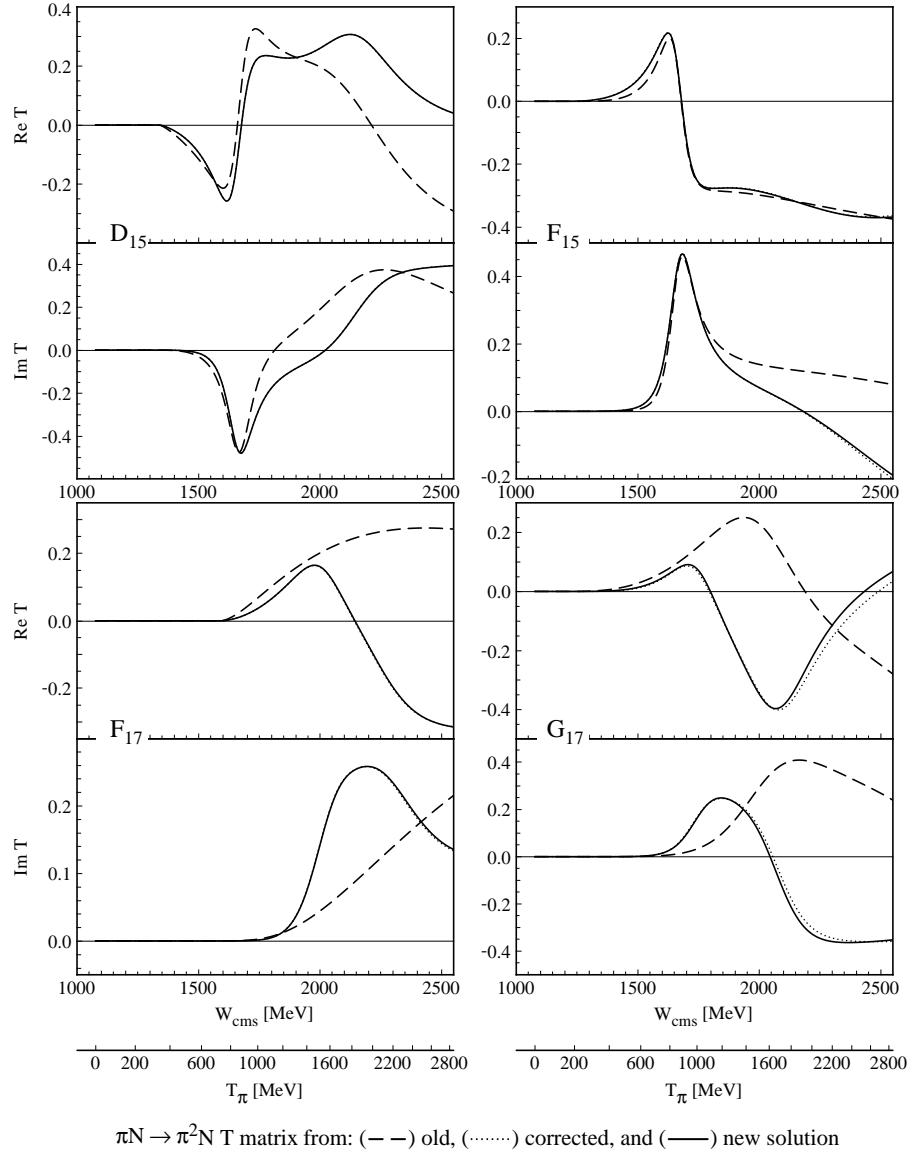
$\pi N \to \pi^2 N$ T matrix from: (− −) old, (⋯⋯) corrected, and (——) new solution

FIG. 11. The $\pi N \to \pi^2 N$ amplitudes in D_{15}, F_{15}, F_{17} and G_{17} partial waves. The meaning of the different curves is given in the caption of Fig.4.